JOURNAL OF GEOPHYSICAL RESEARCH, VOL. 105, NO. A4, PAGES 7491–7508, APRIL 1, 2000

Relationship of halo coronal mass ejections, magnetic clouds, and magnetic storms

D. F. Webb,[1,2] E. W. Cliver,[3] N. U. Crooker,[4] O. C. St. Cyr,[5] and B. J. Thompson[6]

Abstract. Halo coronal mass ejections (CMEs) had been rarely reported in coronagraph observations of the Sun before the Solar and Heliospheric Observatory (SOHO) mission. Since mid-1996, however, the SOHO Large Angle Spectrometric Coronagraph (LASCO) instruments have observed many halo or partial-halo CMEs. A halo CME, especially when associated with solar activity near sun center, is important for space weather concerns because it suggests the launch of a potentially geoeffective disturbance toward Earth. During the post-solar minimum period from December 1996 to June 1997, we found that all six halo CMEs that were likely Earthward-directed were associated with shocks, magnetic clouds, and moderate geomagnetic storms at Earth 3–5 days later. The results imply that magnetic cloud-like structures are a general characteristic of CMEs. Most of the storms were driven by strong, sustained southward fields either in the magnetic clouds, in the post-shock region, or both. We discuss the characteristics of the halo events observed during this period, their associated signatures near the solar surface, and their usefulness as predictors of space weather at Earth.

1. Introduction

Coronal mass ejections (CMEs), vast structures of plasma and magnetic fields that are expelled from the Sun, are now known to be a key causal link between solar eruptions and major interplanetary disturbances and geomagnetic storms [*Gosling et al.*, 1991; *Kahler*, 1992]. CMEs moving outward from the Sun along the Sun-Earth line can, in principle, be detected when they have expanded to a size that exceeds the diameter of a coronagraph's occulting disk, which blocks the bright solar photospheric light [*Michels et al.*, 1997]. Since CMEs can be approximated as spherically symmetric structures, CMEs directed toward or away from the Earth should appear as expanding halo-like brightenings surrounding the occulter. Before the SOHO mission, halo CMEs had only infrequently been reported in coronagraph observations of the Sun [e.g., *Howard et al.*, 1982], and the above interpretation had been questioned [*St. Cyr and Hundhausen*, 1988]. However, with the increased field of view and sensitivity of LASCO, such CMEs have been detected at a rate of 1–3 per month during and just after solar minimum. Halo CMEs appear as expanding, circular brightenings that completely surround the occulter, suggesting that they are spherically symmetric structures moving outward along the Sun-Earth line.

The European Space Agency/NASA Solar and Heliospheric Observatory (SOHO) was launched in late 1995 and dwells at the L1 Lagrange point upstream of Earth. The Large Angle Spectrometric Coronagraph (LASCO) instrument is a suite of three coronagraphs on SOHO, called C1, C2 and C3, which together view the corona from 1.1–30 R_s [*Brueckner et al.*, 1995; *Howard et al.*, 1997]. The fields of view of the coronagraphs are C1, 1.1–3, C2, 2–6, and C3, 3.5–30 R_s. In this paper we describe observations made primarily with the C2 instrument but also including the extended views with C3.

A complete halo CME was observed by the LASCO coronagraphs on January 6, 1997, and used to forecast the arrival at Earth on January 10 of a magnetic cloud/flux rope and associated geomagnetic storm (see *Fox et al.* [1998] and associated papers). This prediction was made because the CME was halo-like, there were reports of activity near sun center as viewed from Earth. The predicted transit time to Earth was based on the typical speed of a CME of 450 km s^{-1} (D. Michels, private communication, 1998). This particu-

[1]Institute for Scientific Research, Boston College, Newton Center, Massachusetts.

[2]Also at Air Force Research Laboratory, Hanscom Air Force Base, Massachusetts.

[3]Air Force Research Laboratory, Hanscom Air Force Base, Massachusctts.

[4]Center for Space Physics, Boston University, Boston, Massachusetts.

[5]CPI/Naval Research Laboratory, NASA Goddard Space Flight Center, Greenbelt, Maryland.

[6]NASA Goddard Space Flight Center, Greenbelt, Maryland.

Paper number 1999JA000275.
0148-0227/00/1999JA000275$09.00

lar event was important because it was the first time that a halo CME observed by SOHO had been used to predict a geomagnetic storm. Because the CME arose from near Sun center and occurred near minimum solar activity, its source region could be studied in detail.

During the next few months, a series of halo CMEs were followed 3–5 days later by magnetic clouds observed by the Wind spacecraft upstream of Earth and by moderate storms at Earth, at a rate of about 2 per month. Because of the relative frequency of this activity and the realization that observations of halo CMEs can be useful both for forecasting space weather and better understanding the internal structure of CMEs, we began the study whose results are reported here. Since halo CMEs are indicative of coronal mass and magnetic fields which are launched through the corona along the Sun-Earth line either directly toward or away from the Earth, it is clear that they provide a unique opportunity (1) to evaluate the near-surface sources of CMEs and, subsequently, (2) to measure in-situ their internal structure as they pass over spacecraft near Earth. Our approach to the first goal was to examine the nature and location of all solar activity observed on the solar disk within ~3 hours of the first observation of the halo CME by the LASCO instrument. Our approach to the second goal was to use the solar wind observations to first identify the likely CME structures upstream of the magnetosphere and then to examine and compare potentially geoeffective structures, especially prolonged periods of southward magnetic field, with the ensuing storm activity. During this relatively simple phase of the solar cycle, these tasks proved to be surprisingly straightforward, showing the utility of the halo CME observations both for understanding CMEs and forecasting space weather.

During the 5-month period starting with the January 1997 event, LASCO observed a total of 14 halo CMEs, defined here as CMEs with spans >140°. Seven of these were complete, 360° halos. Five of these events were followed within 5 days by apparent magnetic clouds and storms at Earth. Four of these five events, on January 6, February 7, April 7, and May 12, 1997, have been studied as "Sun–Earth Connection events" under the International Solar-Terrestrial Physics (ISTP) program (see, e.g., the papers in *Geophysical Research Letters, 25,* (14 and 15) 1998). The "official" list of magnetic clouds/flux ropes determined by the Wind Magnetic Fields Investigation (MFI) team also included modeled flux rope events just before and just after this 5-month period, on December 24–25, 1996, and June 8–10, 1997. Since there were no other clouds listed for several months before the December event, we decided to study the full 6-month period from mid–December 1996 to mid–June 1997. Sunspot activity minimum occurred between May and September 1996 [*Harvey and White,* 1999]; therefore, our study period appears to en-

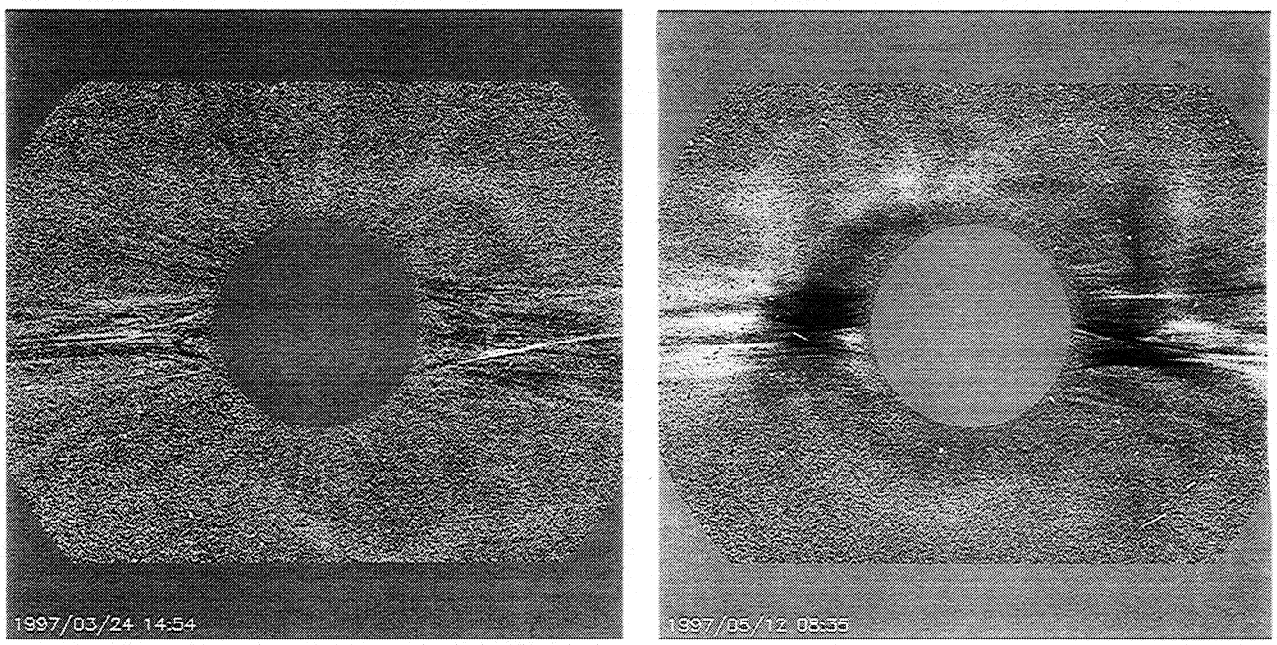

Figure 1. Examples of partial and complete halo CMEs observed by LASCO. Solar north is up and east is to the left (a) Expanding ring-like CME which forms a partial halo extending over 200° of arc around the C2 occulter, on March 24, 1997. This is a difference between direct images at 1454 and 1344 UT. The CME was first detected in C2 at 0737 UT. (b) Expanding CME which forms a complete ring, or halo around the C2 occulter, on May 12, 1997. A difference image, here between images at 0835 and 0735 UT, is again required to see the faint halo CME material. Note the alternating bright and dark structures east and west of the sun, indicating material moving out along the preexisting equatorial streamers in the skyplane, suggesting a toroidal expansion.

compass the first significant, sustained eruptive activity of the new 23rd solar cycle.

Howard et al. [1982] first reported the observation of a halo CME on November 27, 1979, with the Naval Research Lab's Solwind coronagraph. It was associated with a large, sun-centered filament disappearance and flare at the Sun and an interplanetary shock, sudden commencement, and storm at Earth 3 days later. Direct observations of the plasma traveling along the Sun-Earth line were made from the twin Helios spacecraft in solar orbits [*Jackson,* 1985]. Only 2% (~20) of all Solwind CMEs were called "halos," and their average span was 309°, indicating that some were partial-halo CMEs whose central axes were directed off the line of sight.

The SOHO LASCO coronagraphs began observing the Sun in early 1996 and, since mid-1996, have observed many halo or partial-halo CMEs. Examples of a partial and a complete halo CME observed by LASCO are shown in Figure 1. Halos can be either diffuse and featureless around the solar disk, or irregular and asymmetrical. In these examples there is evidence for concentric ring-like structures moving outward. Histograms of the distributions of central latitudes, angular sizes (spans), and speeds of the 104 LASCO CMEs observed during our study period from December 15, 1996, through May 1997 are shown in Figure 2. The angular span distribution is similar to that of all LASCO CMEs from early 1996 through June 1998 and shows two components (St. Cyr et al., Properties of coronal mass ejec-

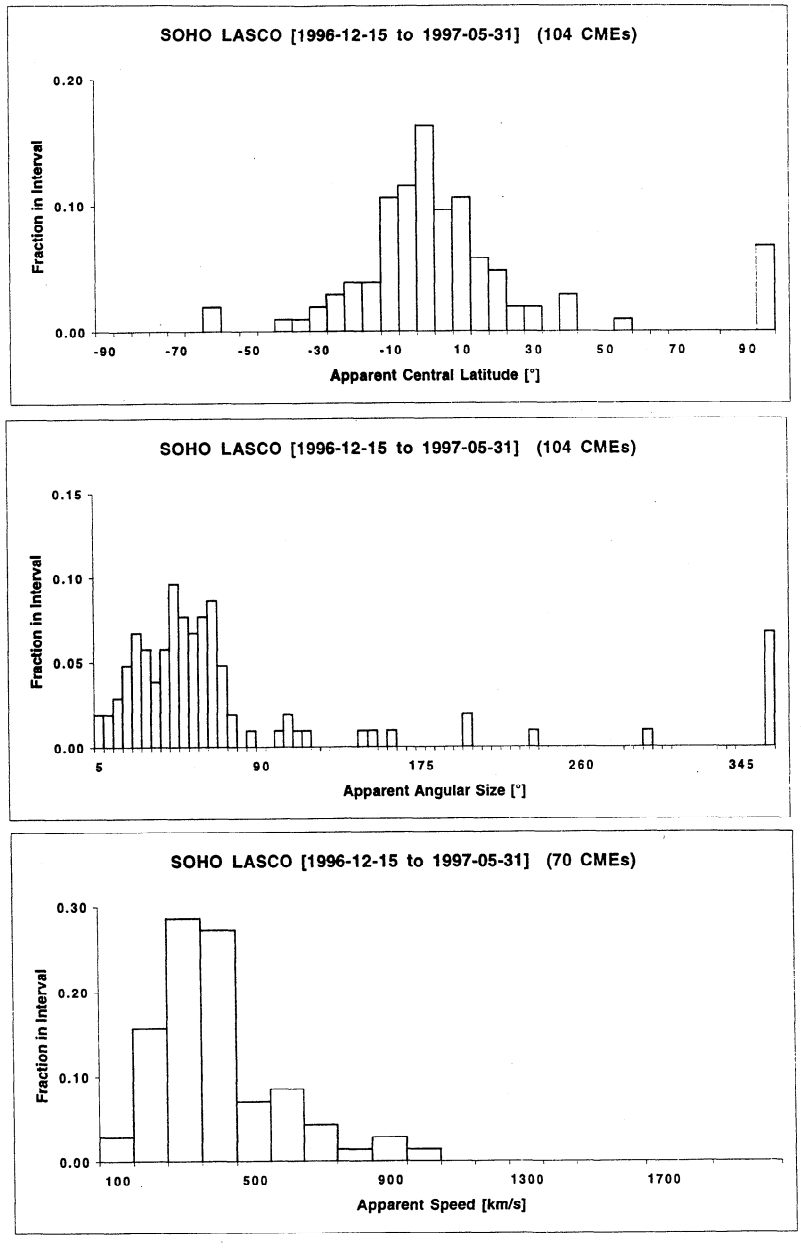

Figure 2. Distribution histograms of (a) the apparent central latitudes, (b) the angular sizes (spans), and (c) the speeds of all (104) LASCO CMEs observed from December 15, 1996, through May 1997.

tions: SOHO LASCO observations from January 1996 to June 1998, submitted to *Journal of Geophysical Research,* 1999). Most CMEs have spans <100° with an average of ~50°. Then there is a long tail in the distribution of CMEs with larger spans out to the complete halos at 360°. For this study we used the convenient break in the two distributions at 140° as the somewhat arbitrary lower limit for defining halo CMEs. We will see that whether the halo CME is geoeffective or not depends somewhat on the value of this lower limit used to define a halo event. Another selection criterion that is being used to define geoeffective CMEs is to include only CMEs whose spans exceed 100° and encompasses one or the other of the solar poles [*Lyons et al.,* 1998].

In the following section we describe the solar activity and source regions associated with the halo CMEs in our study. In section 3 we discuss the associated activity in Earth's vicinity, especially magnetic clouds and their relation to geomagnetic storms. In section 4 we use solar wind measurements to confirm the halo CME–storm associations for these events, and in the last section we summarize the results and their pertinence to space weather.

2. Solar Sources of Activity Related to Halo CMEs

Here we examine the characteristics of the "frontside" activity associated with the halo CMEs in this study. *Hudson et al.* [1998], *Cane et al.* [1998; 1999] and *Brueckner et al.* [1998] performed early surveys of LASCO halo CME events and their associated solar and geomagnetic activity. *Hudson et al.* [1998] studied Yohkoh soft X-ray observations of solar surface activity associated with halo CMEs, and *Cane et al.* [1998; 1999] compared solar wind ejecta signatures with halo CMEs, both during the same period as this study. *Brueckner et al.* [1998] studied the relationship between geomagnetic storms with $Kp \geq 6$ and LASCO CMEs from March 1996 through June 1997. In this paper we present results of a more detailed analysis of the chain of activity linking solar eruptions and storms at Earth, including examinations proceeding in both directions. Preliminary versions of this analysis have been presented at several meetings [e.g., *Webb et al.,* 1997a, 1998a].

Table 1 presents the list of 14 halo CMEs observed by LASCO from mid-December 1996 to mid-June 1997. The time when the CME was first observed in the C2 field of view and its angular span are shown in columns 2 and 3, respectively. Details on the near-surface solar activity that we associated with the onset of each CME are shown in the last seven columns. (This table contains three more halo CMEs than studied by *Hudson et al.* [1998]. These were added after a subsequent reanalysis of the LASCO data by one of us [CST].)

The method that we used to determine whether a particular type of solar phenomenon was associated with a given halo CME was patterned after those used in prior statistical studies of Skylab and SMM CMEs [i.e., *Munro et al.,* 1979; *Webb and Hundhausen,* 1987; *St. Cyr and Webb,* 1991]. Since in a coronagraph a CME cannot be detected until its leading edge has emerged from behind the occulting disk, one must extrapolate back in time and space to the solar surface to search for possibly associated activity. In coronagraphs CMEs appear brightest above the solar limb in the skyplane. However, associating surface activity with such CMEs

Table 1. LASCO Halo CMEs and Associated Solar Activity

CME			Associated Activity						
Date	First Obs., UT	Span, deg.	Flare[a]	Onset, UT	Location	Pol.[b]	DF[c]	Wave	DR[d]
Dec. 19, 1996	1630	293	1F,C2 5hr	1600	S14°W10°	O	Yes	—	2
Jan. 6, 1997	1510	360	– A1 2hr	1400	S24°W01°	N	Yes	—	1?
Feb. 7, 1997	0030	360	– A9 1d.?	6,2300	S25°W30°	N?	Yes	—	~3
Feb. 22, 1997	2330	200	– – –	—	—	—	No	—	0
Mar. 9, 1997	0430	150	– B3 16hr	0340	N03°E75°	O?	No?	—	(1)
Mar. 24, 1997	0737	200	– – –	—	—	—	No	—	0
April 7, 1997	0626	360	– – –	—	—	—	?	—	—
April 7, 1997	1427	360	2N,C7 >8hr	1400	S29°E20°	N	Yes	Yes	2
April 16, 1997	~0735	145	(Sm. events)	—	—	—	No?	No	0
April 27, 1997	0031	233	?sF,B7 1–2hr	?26,2351	?S17°W37°	N	No	No	0
April 27, 1997	1026	360	– – –	—	—	—	No	No	0
April 27, 1997	1459	360	– – –	—	—	—	No	No	0
May 12, 1997	0630	360	1F,C1 14hr	0453	N21°W08°	N	Yes	Yes	2
May 21, 1997	~2100	160	sF,M1 >3hr	<2008	N05°W12°	O	No	Yes	1

[a]Optical importance, GOES X-ray peak flux and duration.
[b]Hale polarity of active region: Old(O) or New(N) cycle.
[c]DF = Disappearing filament.
[d]DR = Dimming region.

is difficult because activity near the limb is poorly observed or might be invisible over the limb. In the previous studies, fixed time windows and spatial (latitude and longitude) ranges were used to define the degree of association of certain types of surface activity with CMEs. In our study of halo CMEs, the association problem is simplified in two important ways. First, if the CME is directed Earthward, any associated surface activity should lie at or within a few tens of degrees of Sun center, even though CMEs can have large spans and associated surface events can be offset from the CME axis [*Webb*, 1992]. Second, our study period was just after the minimum of solar activity, thus greatly reducing ambiguities about the CME associations. In this sense our study was similar to that of *St. Cyr and Webb* [1991], who studied SMM CME associations during the minimum of the last solar cycle.

Therefore, we searched for solar activity within a time period starting ~3 hours before and until the time that the leading edge of the CME was first observed in the LASCO C2 coronagraph at a height of ~1.0 R_S above the limb. We included in our search any activity occurring on the visible disk within this time window. The type of activity we examined was the same as that searched in the aforementioned studies. These included erupting prominences, optical (Hα) flares, soft X-ray events, and metric radio type I, II, or IV bursts. Most of these activity types are listed in the monthly Solar Geophysical Data Bulletins [1996–1998]. For our study we had additional data available in the form of Yohkoh Soft X-ray Telescope (SXT) and SOHO Extreme ultraviolet Imaging Telescope (EIT) images for general activity searches. These data were also used to search during each event window for coronal dimming regions and waves, both of which are now considered to be physically associated with CMEs (see below).

Of the 14 halo CMEs, we concluded that seven had probable frontside surface activity. This is as expected, since half of all halo CMEs should be aimed Earthward (frontside) and half away from Earth (backside). As discussed above, the association of these events with the CMEs was fairly unambiguous since all seven events began within 2 hours of the first CME observation and there was no other activity on the visible disk during the time period. We note that the January 6 surface activity was very weak and would not have been considered to be CME-associated if the geoeffective halo CME had not been observed [*Webb et al.*, 1998b].

Three of the other halo events were preceded by possible frontside activity, which we now think was not associated with the halos. The first of these, on April 7 at 0626 UT, was a very faint complete halo. A small flare with an EIT wave starting on April 6 at 2350 UT in the same active region associated with the later large April 7 halo CME was probably too early to be associated with the first CME observed at 0626. There were several small flares associated with the lone active region on the disk near Sun center before the partial halo CME on April 16. However, since these events were not reported as optical flares and their peak GOES X-ray levels were barely above the A7-level background early on this day, it is unlikely that they were associated with the CME. Finally, three halo CMEs were observed on April 27. The first closely followed a small flare starting on April 26 at 2351 UT in the only region on the disk that showed activity during this period. However, this region was fairly far to the southwest of disk center and was very small, and all the activity from the region during this period was minor and of a confined nature. Thus, we feel that all three halo CMEs on April 27 probably originated on the backside of the Sun.

The source regions of the seven frontside halo CMEs generally were associated with flares in small active regions within about 0.5 R_S, or 40° of Sun center [cf. *Hudson et al.*, 1998]. The peak soft X-ray fluxes of the flares ranged over 3 orders of magnitude, and the flares were of relatively long duration, from 2 hours to a day. Five of the seven source flares were also associated with disappearing filaments (labeled "DF" in Table 1), and in four cases these were of major importance, Importance 2 or 3. (The Importance level of a filament disappearance is defined in terms of the length of the preexisting filament, Solar-Geophysical Data Bulletins, 1997). All of the flares having sufficient EIT data coverage (3 of 7) were accompanied in the corona by circular, expanding wavelike emission and dimming of preexisting emission.

To date well-defined, large-scale coronal "waves" have only been detected in the EUV by the SOHO EIT instrument after March 1997. Before then the EIT data cadence was usually too low to detect such fast moving features. Since early April, images have routinely been obtained in the 195Å passband filter of EIT, which is dominated by emission lines of FeXII (1.5×10^6 K), at a typical cadence of 3-4 images per hour, and many EUV waves have been identified [*Thompson et al.*, 1999a]. In Table 1, after March 1997, EIT waves were observed for all three of the frontside halo CME source regions. (To the contrary, *no* such waves were observed for the other April events, thus supporting our conclusion that those were backside halo CMEs.) Particularly clear waves were associated with the complete halo CMEs on April 7, 1997 [*Thompson et al.*, 1999b], and May 12, 1997 [*Thompson et al.*, 1998]. The EIT events consist of a rim of enhanced coronal emission traveling quasi-radially across the disk from the flare site. Figure 3 shows the coronal wave observed during the May 12 event. Although a detailed understanding of these events is not yet available, they are thought to be caused by fast-mode MHD waves that may or may not steepen into shock waves. Those EIT waves which steepen into shocks, as evidenced by an association with radio metric type II bursts, may be similar to the rare "Moreton" waves observed in the photosphere and chromosphere. Although the physical relationship of the EIT events to CMEs has yet to be determined, preliminary surveys indicate that there may be a strong association between the two phenomena [*Thompson et al.*, 1999a]. This correspondence is supported by our limited data set.

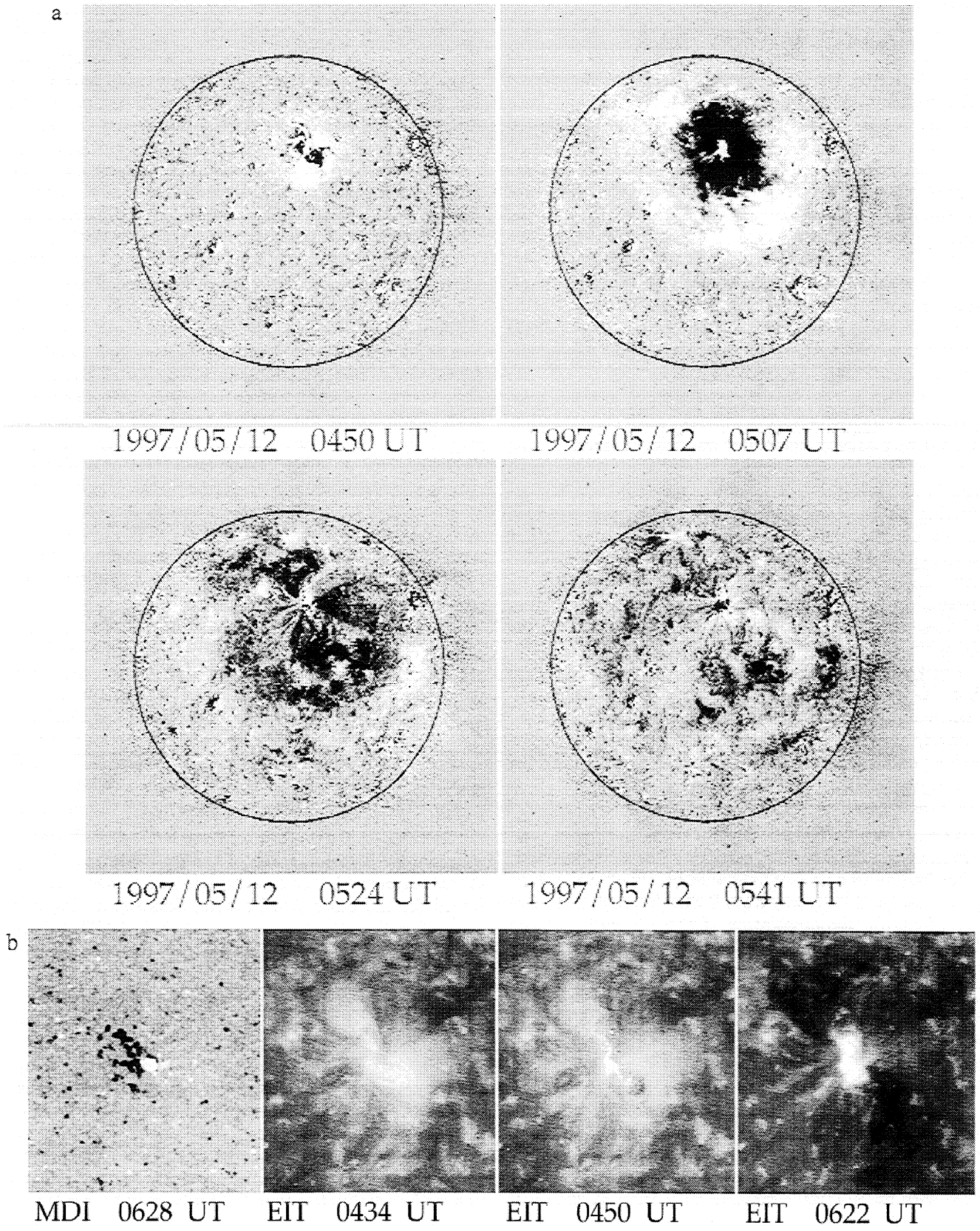

Figure 3. Example of surface activity associated with the May 12, 1997, halo CME. (a) SOHO/EIT images of large-scale coronal wave. These are differences between consecutive pairs of full-disk 195Å images; the later image time is listed. (b) Development of the coronal LDE arcade and dual flanking dimming regions. The first image is a SOHO/Michelson-Doppler Imager (MDI) photospheric magnetogram. The other three images are 195Å EIT images showing at 0434 UT the preexisting active region, at 0450 UT the event onset, and at 0622 UT the fully developed arcade and dual dimmings. During the onset a filament was beginning to erupt from the southern part of the region. Adapted from *Thompson et al.* [1998].

All of the halo CMEs associated with probable frontside activity were also accompanied by small, long-duration ($\geq$2 hour) coronal arcades and adjacent dimming regions as viewed in EUV by EIT (this study) or in soft X-rays by the Yohkoh SXT [*Hudson et al.*, 1998]. Figure 3b illustrates the arcade–dimming pattern for the May 12, 1997, event. Such coronal arcades are a well-known surface signature of CMEs [*Kahler*, 1977; *Sheeley et al.*, 1983; *Webb*, 1992] and suggest the eruption and subsequent reconnection of the strongest magnetic field lines in the source regions associated with the CME. The dimming regions imply that material is evacuated from the low corona, and a few estimates show that the amount lost may be a significant fraction of the mass which later appears in the white light CME [see *Hudson and Webb*, 1997]. In some cases, such as the May 12 event, symmetric dimmings occur in regions which may be of opposite magnetic polarity flanking the central arcade. This suggests that these regions mark the feet of a flux rope that is expanding into the solar wind, an idea supported by the observations of associated flux-rope magnetic clouds at Earth [e.g., *Smith et al.*, 1997; *Sterling and Hudson*, 1997]. In Table 1 the number of separate dimming regions in each event is shown in the "DR" column: Four of the seven frontside source regions were accompanied by multiple dimming regions.

Stacked synoptic maps of the photospheric magnetic field are shown in Figure 4 for the six consecutive solar rotations, CR 1917-1922, during which the seven frontside halo CMEs occurred. The likely solar source regions of the CMEs (Table 1) are circled on each map. The light and dark gray shadings show the large-scale weak photospheric magnetic fields of positive and negative polarity, respectively. For the current (23rd) solar cycle, positive field is dominant in the Northern Hemisphere and negative in the Southern Hemisphere. Thus, the boundaries between these regions trace the magnetic polarity inversion, or "neutral lines," on the surface. The white and black regions denote the strongest active region fields. Regions with the Hale polarities typical of the old activity cycle (22nd) have negative (black) polarity leading in the north and trailing in the south. Those with polarities typical of the new cycle (23rd) are the opposite. The Hale polarities of the associated active regions are listed in column 7 of Table 1 as of Old(O) or New(N) cycle. The white lines are the boundaries of coronal holes as measured on He–I 10830Å images.

Of particular note is the nearly complete southern neutral line which encircles the Sun at $\approx$50° latitude. This neutral line forms the locus of the southern polar crown of filaments which typically resides at 50° latitude during sunspot cycle minimum [see *Webb*, 1998, Figure 4]. Most of the important solar activity in 1996 and early 1997 occurred in the Sun's Southern Hemisphere [Solar-Geophysical Data Bulletins, 1997–1999]. The January and February 1997 events (during CR 1918 and 1919, respectively) occurred along the same branch of the polar crown neutral line at longitude $\approx$330° where it bent sharply to the north. The December and April events occurred along or near a similar northward bend in this same neutral line at $L \approx$210–240°. Earlier, the adjacent region at $L \approx$240–280° was the site of a single active region or zone which dominated solar activity from the time of its birth in May to the end of 1996. Most of the major activity in late 1996 arose from this vicinity [e.g., *Benevolenskaya et al.*, 1999], including the well-studied flare/CMEs on September 25–27 and October 5, 1996.

At the time of the events discussed in this paper, this region was decaying, and new-cycle regions had begun appearing, first in the Northern Hemisphere then in the Southern Hemisphere. The source regions of the January 6, April 7, and May 12 events on CR 1918, 1921, and 1922, respectively, were of new-cycle polarity, while those of the December 19 and May 21 events on CR 1917 and 1922, respectively, were old cycle. The February 7 event involved a large filament eruption rather than an active region, and the March 9 active region was nearly on the equator, making its Hale polarity indeterminate.

In summary, the solar activity associated with the seven frontside halo CMEs had these typical characteristics: (1) complete or large-arc CMEs arising from surface activity within $\sim 0.5 R_S$ of Sun center suggesting eruptive events aimed toward Earth; (2) surface events consisting of long-enduring coronal arcades that, with the exception of the May 21 event, were not energetic (GOES peak fluxes of A1–C7) and occurred in small emerging or rapidly evolving active regions; (3) coronal dimming regions that were likely density depletions; (4) large-scale coronal (EIT) waves; and (5) in most cases, small erupting filaments.

3. Activity at Earth Associated With the Halo CMEs

3.1. Comparisons With Solar Wind and Geomagnetic Activity

We studied the geoeffectiveness of the frontside halo CMEs in our sample by examining data from the Wind spacecraft at 1 AU and geomagnetic activity at Earth over an interval 3–5 days after the onsets of the halo CMEs. This delay, or transit time, for the disturbance to travel from the Sun to Earth was chosen because the average solar wind speed of 450 km s^{-1} yields a transit time to 1 AU of 4 days, and such speeds are typical of CME material detected in the inner heliosphere [*Webb and Jackson*, 1990] and of transient events observed in situ at 1 AU [*Gosling*, 1996]. In several cases these associations were confirmed by observations of interplanetary emission at decimetric and kilometric radio wavelengths by the Wind/WAVES radio experiment [e.g., *Reiner et al.*, 1998; *Berdichevsky et al.*, 1998].

In order to more clearly examine the relationship between the halo CMEs and geomagnetic storms, we produced the stackplot of seven consecutive Bartels rota-

tions of the *Dst* index shown in Figure 5 [cf. *Crooker et al.*, 1996]. Such plots are keyed to the 27-rotation rate of the Sun and usually are used to show evidence of recurrent solar activity in solar wind parameters. They are similar to the solar magnetic field plots in Figure 4, except that the solar plots start on different dates and time runs from right to left. The *Dst* index gives the strength of the averaged depression of Earth's magnetic field at the equator and is a commonly used measure of the strength of magnetic storms. Storm-related depressions in *Dst* are usually considered to be caused by the growth of the Earth's ring current. Solid triangles at the bottom of each rotation mark the peak times of storms having a depression in *Dst* of at least −50 nT; this level is used to define moderate-sized magnetic storms [e.g., *Loewe and Prolss*, 1997]. Of the 12 storms so defined during this interval, only two, on April 22 and May 15, 1997, exceeded the −100 nT *Dst* level defining strong storms.

The onset times at the Sun of the 14 halo CMEs from Table 1 are denoted in Figure 5 by vertical bars: solid lines are for the seven probable frontside events, and dashed lines are for the seven possible or probable backside events. The shading on the plots roughly indicates the sectors of dominant polarity of the interplanetary magnetic field (IMF) at Wind; white is "away" from the Sun or positive, and gray is "toward" the Sun or negative. Brief periods of apparent mixed polarities are not marked on Figure 5. Finally, the occurrence and durations of magnetic cloud structures detected in Wind data are indicated by the horizontal, filled black bars. These have been defined in two ways. First, five of these structures are definite magnetic clouds in that they have been successfully fit by a force-free flux rope model [*Lepping et al.*, 1990] (see Wind/MFI Team list at http://-lepmfi.gsfc.nasa.gov/mfi/mag_cloud_pub1p.html). The other three, on February 10, April 11, and May 26–27, are considered cloud-like in that they have some characteristics typical of magnetic clouds [*Burlaga*, 1991] but do not fit the simple flux rope model.

Statistically we find from Figure 5 that 9 of the 12 moderate storms during this period were preceded within 5 days or less by halo CMEs. In the opposite sense, 12 of the 14 halo CMEs that occurred during

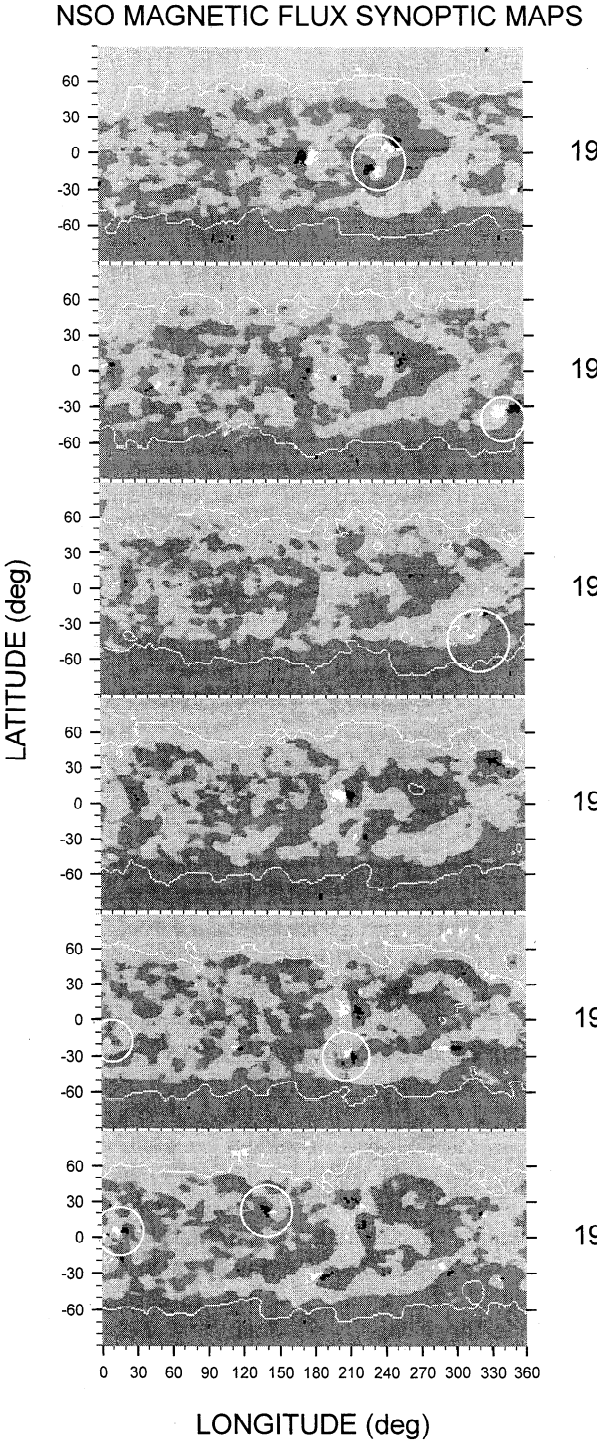

Figure 4. Stacked synoptic maps of the photospheric magnetic field for the six consecutive solar rotations, CR 1917–1922, involving the seven frontside halo CMEs (Table 1). The likely solar source regions of the events are circled on each map. The light and dark gray shading show the large-scale weak fields of positive and negative polarity, respectively; positive field is dominant in the Northern Hemisphere, and negative is dominant in the Southern Hemisphere. Thus, the boundaries between these regions trace the polarity inversion, or "neutral lines," on the surface. The white and black regions denote the strongest positve and negative fields, respectively, i.e., active regions. Regions with the Hale polarities typical of the old 22nd activity cycle have negative (black) polarity leading in the north and trailing in the south; those on CR 1917 are an example. Those with polarities typical of the new 23rd cycle are the opposite, for example, the source regions of the January 6, April 7, and May 12 events on CR 1918, 1921, and 1922, respectively. The white lines are the boundaries of coronal holes as measured on He–I 10830Å images. Maps are courtesy of J. Harvey, National Solar Observatory-Kitt Peak.

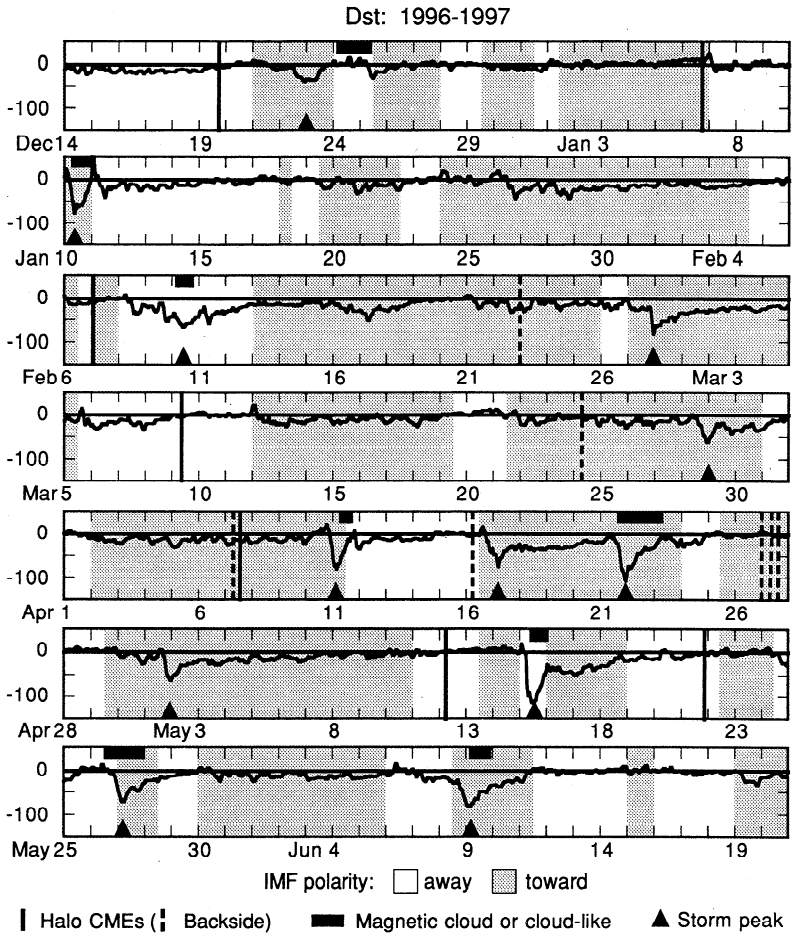

Figure 5. Stackplot of seven Bartels rotations (Numbers 2231–2237) of the *Dst* level (nT, left scale) showing geomagnetic storms at Earth. The horizontal line marks the zero nT level. The occurrences at Wind of magnetic clouds or cloud-like structures are denoted by the horizontal bars above the zero line on each rotation. Vertical lines mark the onsets at the Sun of LASCO halo CMEs: Solid lines are probable frontside events, and dashed lines are probable backside events. Solid triangles mark the peak times of moderate storms, i.e., $Dst < -50$ nT.

this period were followed within ~5 days by a moderate storm. This appears to be a remarkably high correspondence, considering that only half of the halo CMEs were possibly aimed at Earth. We will return to this subject in section 3.2.

Table 2 compares the seven probable frontside events from Table 1 with the occurrences of solar wind transient activity at 1 AU in the Wind data and moderate magnetic storms. The first three columns repeat the halo CME date, first observed time, and span from Table 1. Column 4 gives the radial vector distance from the geometrical center of the Sun to the assumed source region. This provides a crude measure of how far from the Sun-Earth line the CME launch site might be. In all cases except January 6 and February 7, this is the radial distance of the associated active region from Sun center at the time of the event (see Figure 4). On January 6 the halo CME was associated with a small erupting filament and a brightening plage region; the specified distance is measured from the filament site. On February 7 the CME was associated with a small active region and a large erupting filament on the southwestern disk and, later, a very long, narrow arcade outlining the preexisting southern neutral line. The first distance given is from the active region, and the second is from the closest point of the arcade to Sun center. Columns 5 and 6 give the date and time of any shock and of any magnetic cloud structure at 1 AU at Wind that we associate with the given halo CME. The last two columns give the peak *Dst* value of the ensuing geomagnetic storm and the transit time in days between the onset time of the surface source activity at the Sun (Table 1) and the storm peak at Earth.

A major difficulty in using halo CMEs to forecast space weather is a lack of knowledge of the true speed of the CME. The speeds of CMEs are derived from height-time plots, usually of their leading edge along a line of radius. These speeds are thus as projected in

Table 2. Frontside Halo CMEs and Associated Geoactivity

CME				Associated 1 AU Activity			
Date	First Obs., UT	Span, deg.	Dist., R_S	Shock,[a] day, hour	Cloud,[a] day, hour	Storm Peak, *Dst*	TT,[b] days
Dec. 19, 1996	1630	293	0.26	[No;	?	−41;	3.3]
				?(23, 15)	24, 03	−33	4.4
Jan. 6, 1997	1510	360	0.29	10, 01	10, 0440	−78	3.9
Feb. 7, 1997	0030	360	0.56; 0.65	9, 1245	10, 0240	−68	3.5
Mar. 9, 1997	0430	150	0.76	No	No?	No	—
April 7, 1997	1427	360	0.50	10, 1255	11, 06	−82	3.6
May 12, 1997	0630	360	0.40	15, 0455	15, 01	−115	3.3
May 21, 1997	≤2100	160	0.23	25, 1350;	?		
				26, 09	26, 09	−73	5.4

[a]Times are for onsets of shocks and magnetic clouds at Wind spacecraft.
[b]Transit time from solar onset to storm peak at Earth.

the skyplane. For a CME whose central axis is above the solar limb and, therefore, in the skyplane, the measured speed is a good approximation of the true speed. However, in the case of a halo CME, the true leading edge speed cannot be measured because the axis of the CME is 90° away from the skyplane and occulted by the coronagraph. The projected speed that is measured is related somehow to the expansion of the sides of the CME and its relation to the true leading edge speed is unknown. Therefore, we did not use the measured speeds of the halo CMEs in associating them with transients at 1 AU. Instead, we searched for such activity 3–5 days after the halo onset time and then calculated the solar source-to-transient activity transit time. We then compared these transit speeds with the in-situ solar wind speeds of the magnetic clouds at 1 AU that followed each of the six frontside halo CME events with near-Sun center sources. The transit and in-situ speeds of these events all agreed to within 100 km s^{-1} of each other, thus supporting their physical association. However, as expected, the measured CME "speeds," which varied from 80-805 km s^{-1}, were not correlated with the transit speeds.

The table shows that all but one of the seven frontside halo CMEs were associated with transient structures in the Wind data. The exception was the March 9 event, which was a partial halo of 150° spanning mostly the east limb and whose source region was 75° east of central meridian. We included this event in the comparison study for completeness because the source region was visible on the frontside of the disk. The source regions of the other six halo CMEs were at distances of 0.23–0.56 R_S from Sun center. All six of these CMEs were followed by a magnetic cloud or cloud-like structure at Wind within 5 days of onset. These clouds had peak magnetic flux amplitudes of 9–25 nT and durations of 13–32 hours. A magnetic cloud, or at least a cloud-like feature, was identified using the usual definition of a smooth, long-lasting enhancement in the field magnitude coincident with a smooth rotation of the field in at least one axis [e.g., *Burlaga,* 1991]. Three of these magnetic clouds were well fit by a force-free flux rope model (R. Lepping, private communication, 1998). Five of the six clouds were preceded by an interplanetary shock at Wind (Berdichevsky D., A. Szabo, R. P. Lepping, F. Mariani and A. F. Vinas, Interplanetary fast shocks and associated drivers observed through the twenty-third solar minimum by Wind over its first 2.5 years, submitted to *Journal of Geophysical Research,* 1999). The exception was the December 24–25, 1996, cloud which was preceded on December 23 at 1500 UT by a density increase that may have been a weak shock. The May 26–27, 1997, cloud was preceded by two shocks. There is evidence in the solar wind data that both the December and May 26–27 flux ropes closely followed earlier transient structures. We discuss these double structures in section 3.2.

At Earth all six of the halo CME–magnetic cloud events were followed by geomagnetic storms. These storms had peak *Kp* levels of 4 to 7− and peak *Dst* levels of −41 to −115. The December 1996 post-CME period actually had two small storms, both with peak levels lower than our original selection threshold for moderate storms of *Dst* = −50 nT. It is likely that only the second, smaller storm was due to the magnetic cloud on December 24–25. The peak *Dst* level of these storms might have been depressed due to the well-known seasonal effect characterized by weaker geomagnetic activity at the solstices.

The May 12–15, 1997, event is the cleanest example of the geoeffectiveness of halo CMEs. The halo CME on May 12 completely surrounded the occulting disk and was first seen in LASCO C2 at 0630 UT (Figure 1b). The height–time profile of its leading edge extrapolated back to Sun center at about the onset time of the only major flare on this day, in active region

8038 at N21°W08°. The X-ray flare had a smooth long-duration profile in GOES of ~1400 hours. This emission arose from a small, bright arcade that formed over a classic filament eruption with expanding double ribbons in the Hα line. The flare was accompanied by a circular EUV wave, and the arcade was flanked northeast and southwest by two dimming regions of the transient-coronal hole type (Figure 3). Region 8038 appeared as a new, rapidly developing region on CR 1922 of new-cycle polarity. It was the only active center on the disk and the site of all flaring activity for several days around May 12.

Figure 6 is a stackplot of key IMF and plasma parameters from the Wind spacecraft for May 14–17, 1997. From top to bottom are plotted the magnetic field amplitude, azimuthal angle ϕ, polar angle θ, the plasma proton density, thermal and bulk speeds, the north–south IMF component B_z (GSM coordinates), and the *Dst* index at Earth. An interplanetary shock arrived at Wind on May 15 at 0115 UT (vertical dashed line), followed 8 hours later by a "classic" magnetic cloud. The shaded region denotes the boundaries of the flux rope modeled by the MFI team (see *Webb et al.* [2000] for a description of the development of this cloud). The transit times between the onset at the Sun of the disturbance and the shock and cloud onset times at 1 AU were 68.0 and 76.0 hours, yielding average transit speeds of 613 and 548 km s^{-1}, respectively. The latter value can be compared to the solar wind speed in the cloud, which increased from 430 km s^{-1} at the front of the cloud to 500 km s^{-1} at its rear. The cloud was in the middle of a toward polarity sector and apparently was being compressed from behind by a high-speed stream (Figure 5). The axis of the fitted flux rope lay nearly in the ecliptic plane such that the strongest field rotation was in latitude. There were strong N to S fields in the compressed region behind the shock, then mostly S to N fields in the flux rope. Note the close correspondence in timing and profile shape of the *Dst* storm signal with the occurrence of these strong, sustained southward ($-B_z$) fields, and increasing wind speed in the cloud. The flux rope had a diameter of 0.20 AU, an axial magnetic flux of 7.35 × 10^{20} Mx, and left-handed twist. The left-handedness of the rope agrees with that expected for Northern Hemisphere filaments and was of the south-east-north (SEN) type as predicted by *Bothmer and Rust* [1997] for this phase of solar cycle 23.

The characteristics of the May 12 source region were very similar to those on April 7 except that the latter region was farther from Sun center, to the southeast. Although both a shock and magnetic cloud arrived at Wind 4 days later on April 11, the cloud could not be fit by a simple rope model, possibly because Wind was too far west of the cloud axis. Likewise, the February 7 filament eruption/arcade was well south and west of Sun center, and the ensuing magnetic cloud at Wind could not be fit by the model. However, the source regions of both the December and January events were close to Sun center and associated with flux rope-fitted clouds at Wind The regions were in the Southern Hemisphere, consistent with the right-handed twist of the ropes.

The January 1997 event was the first Sun-Earth connection event to be studied by the ISTP constellation of

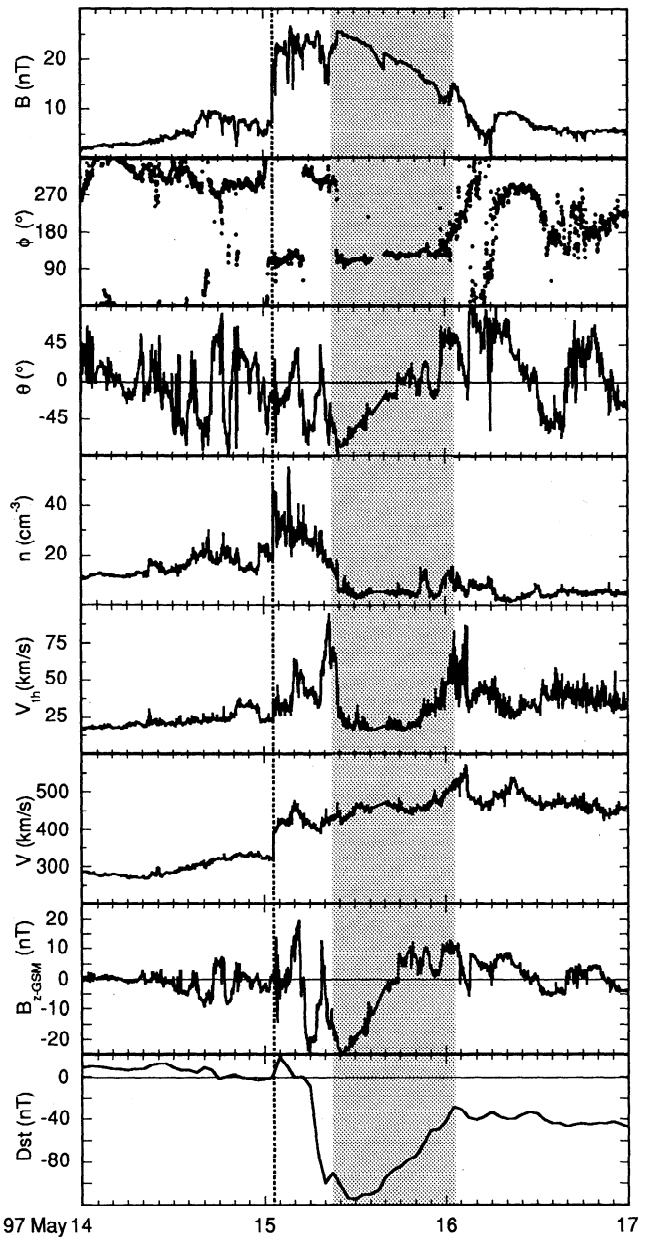

Figure 6. Stackplot of IMF and plasma parameters from Wind for May 14-17, 1997. From top to bottom are plotted the magnetic field amplitude, azimuthal angle ϕ, polar angle θ, the plasma proton density, thermal and bulk velocities, the north–south IMF component B_Z (GSM coordinates), and the *Dst* index at Earth. The vertical dashed line is the time of shock arrival at Wind, and the shaded area denotes the boundaries of the flux rope modeled by the MFI team. Note the close correspondence of the *Dst* storm signal with the occurrence of strong, sustained southward field and increasing wind speed. Wind data are courtesy of R. Lepping and K. Ogilvie, NASA/GFSC.

spacecraft (see *Fox et al.* [1998] and associated papers). The solar and interplanetary circumstances were discussed by *Burlaga et al.* [1998] and *Webb et al.* [1998b]. A small filament disappearance in the southern solar hemisphere was followed by the appearance of the halo CME. A shock arrived at Wind 83 hours later followed by a magnetic cloud and CME ejecta. An unusual feature of the ejecta was a narrow, very dense "plug" of material at the trailing edge of the magnetic cloud, followed by an interface region and a high-speed stream. The main geomagnetic storm mirrored the passage of the cloud observed at Wind, and the trailing high-pressure region compressed the Earth's magnetopause to within geosynchronous orbit. The dense plug contained material at low proton and electron temperature as well as unusual ion charge states, indicating that it was probably remnants of the filament in the trailing part of the CME.

A similar, but extended period of dense, cool material within a magnetic cloud was also observed in ACE and Wind data on May 2–3, 1998, following an erupting filament–halo CME on April 29 [e.g., *Gloeckler et al.*, 1999; *Skoug et al.*, 1999]. Several other recent halo CME–cloud events have had similar solar wind signatures, including the April 7–11 event of our study. Like January, the April event contained a high-pressure region at the trailing edge of the cloud, followed by an interface region and a high-speed stream which compressed the magnetosphere [*Berdichevsky et al.*, 1998]. It is clear that halo CMEs provide us with a unique opportunity to better understand the internal structure of CMEs.

3.2. Solar Wind Drivers of the Geomagnetic Storms

We noted above that 9 of the 12 moderate-level storms which occurred during our study period were preceded within 5 days by halo CMEs. Six of these nine halo CMEs were considered frontside events aimed along the Sun-Earth line and were associated with magnetic clouds at 1 AU just before or during the storms. As is well known, moderate to large storms are well correlated with prolonged periods of southward IMF, and also may be associated with periods of enhanced solar wind speed and density [e.g., *Burton et al.*, 1975]. In this section we first evaluate which portions of the transient ejecta in the Wind data at 1 AU associated with the frontside halo CMEs are responsible for the storms. Then, for completeness, we examine the Wind data around the times of the remaining six storms to determine the geoeffective sources in the solar wind for these events.

Table 3 summarizes our results for the interplanetary sources of the 12 storms. The first column lists the peak date and time of each storm. The middle column is a brief summary of the geoeffective solar wind sources as well as related structures. In the third column we list the most likely associated solar source CME and/or disappearing filament (DF) with the day and hour of onset, and in the last column we give the transit time in days from solar onset to storm peak. The parentheses indicate less likely associations, usually because the halo CMEs were assumed to be launched from the backside and the travel times were very long.

As noted earlier, the six storms associated with frontside halo CMEs were all accompanied by Wind magnetic clouds, and five of these were preceded by shocks. In all these events the *Dst* storm periods closely matched periods of strong, sustained southward fields either in the turbulent regions between the shocks and clouds, in the clouds themselves, or both. The latter case is exemplified by the May 15 storm (Figure 6) in which the initial *Dst* decrease tracked the southward turning of the IMF 4 hours after shock passage, then reached minimum in response to the strong southward field in the leading half of the cloud. Strong B_S fields in both post-shock regions and clouds also were the primary causes of the January 10, February 10, and May 27 storms. The April 11 storm was mostly driven by post- shock southward fields because the cloud field was predominately northward throughout. The cloud appeared to carry the sector boundary change at the start of a high-speed stream.

The December 23–25, 1996, and May 27, 1997, halo CME-related storms may have been associated with twin transients in the solar wind, each with lagging magnetic clouds. In December, each transient had moderate southward fields which caused small storms. The B_S field in the first transient followed a sector boundary and had cloud-like characteristics. The second transient was a flux rope with the field rotating from north to south; its slower transit time suggests that this is the structure most likely associated with the halo CME on December 19. It is possible that this double structure was due to the Wind spacecraft passing through both legs of a single distorted flux rope structure, such as modeled by *Crooker et al.* [1998].

The magnetic cloud on May 26–27 was preceded by two shocks 20 hours apart. The second shock was followed by strong B_S fields in the sheath and cloud which drove the storm. It is unclear whether one or both of these transients were associated with the halo CME late on May 21. The transit time from the CME onset to the cloud and storm peak was slow, 5.4 days. However, although the CME source region was near Sun center, the CME itself as observed by the LASCO C2 coronagraph was unusual. It was the prototype of a class of "toroidal" halo CMEs as defined by *Brueckner et al.* [1998, Figure 1, panel 4]. Simultaneous activity was confined to the equator over both limbs of the Sun, with a faint band connecting them to the south. One interpretation is that the CME consists of a toroid surrounding the solar equator and expanding in all directions. Depending on preexisting structures, transient material from such a CME could reach Earth from a wide range of source longitudes causing unusually prolonged effects.

The remaining six storms could not clearly be associated with any halo CME events. But surprisingly, two of these six storms were driven by magnetic clouds

Table 3. Interplanetary Sources of the Moderate Geomagnetic Storms

Storm Peak (Day; hour)	Southward IMF and Associated Activity[a]	Associated Solar Activity (CME, DF[b], day, hour)	Transit time (days)
Dec. 23, 1996, 00	Medium Bs field following SB; MC?	?	(3.3)
Dec. 25, 1996, 13	Flux rope with trailing Bs field; spiky enhanced density.	Partial Halo, DF. 19,16	4.4
Jan. 10, 1997, 10	Shock 10,01. Strong Bs field in sheath, then S-N in flux rope; big density and IMF enhancement at rear; HSS follows.	Halo, DF. 6,14	3.9
Feb. 10, 1997, 11	Shock 9,13. Strong Bs field in sheath then in MC; low density but peaks at rear; in HSS?	Halo, DF. 6,23	3.5
Feb. 28, 1997, 00	Two shocks: 26,12 and 27,17.5? Strong Bs field and density after SB on 2,27-28; HSS follows.	(Backside Partial Halo. 22,23.5)	(4.7)
Mar. 29, 1997, 00	Medium sustained period of Bs field after high speed; small MC or interaction region?	(Backside Partial Halo. 24,08)	(4.7)
April 11, 1997, 05	Shock 10,13. MC carries SB at start of HSS; strong Bs field in sheath, Bn in MC.	Halo, DF. 7,14	3.6
April 17, 1997, 06	Spiky Bs field associated with SB and interaction region; HSS follows.	None	---
April 22, 1997, 00	Large flux rope with dense front and medium, sustained Bs field (S-N); trails above HSS.	(Backside Partial Halo. 16,07.5)	(5.7)
May 2, 1997, 01	Shock 01,12. Medium spiky Bs field with strong density and IMF in CIR; HSS follows.	(3 Backside? Halos. 27,00.5-27,15)	(5.0)
May 15, 1997, 13	Shock 15,01. Strong, sustained Bs field in sheath then S-N in flux rope; strong density and IMF at start of HSS.	Halo, DF. 12,05	3.3
May 27, 1997, 07	Two shocks 25,13 and 26,09. Second has strong Bs field in sheath and MC; enhanced density at front of MC.	Partial Halo. 21,20	5.4
June 9, 1997, 05	Medium, sustained Bs field in large S-N flux rope; enhanced density in middle.	(None, DF. 6,>07)	(2.9)

[a] IMF, interplanetary magnetic field; SB, sector boundary; MC, magnetic cloud; HSS, high speed stream; CIR, corotating interaction region.
[b] DF, disappearing filament.

with flux rope characteristics! These two clouds, on April 22–23 and June 9, could not be associated with a halo or any other CME up to 5 days earlier. A backside partial halo CME preceded the April event by 5.7 days. A small filament disappeared on the frontside disk 2.9 days before the June cloud, but this transit time seems too fast for such a small event. Including these two cloud events, we can say that 8 of the 12 moderate storms occurring during this period were caused by strong, sustained southward fields associated with magnetic clouds or the post-shock regions preceding them.

What then were the geoeffective sources of the remaining four geomagnetic storms? Three of the four, on February 28, April 17, and May 2, appeared to be associated with southward fields in corotating interaction regions (CIRs) preceding high-speed streams. The *Dst* plots during these events (Figure 5) show the classic profile of peak *Dst* activity followed by low-level, sustained activity for days. The peak activity is caused by compression of preexisting southward fields in the CIR and the sustained activity to southward IMF in Alfvenic fluctuations in the high-speed flow. The sustained activity for these three springtime streams might have been enhanced by the seasonal effect. The peak CIR activity can also be enhanced by CME-related transients, as appeared to be the case for the halo CME–storms on January 10, February 10, April 11, and May 15, 1997, each of which was followed by a period of high-speed flow and sustained *Dst* activity (Figure 5) [cf. *Crooker and McAllister*, 1997]. The frequency of the CIR–high

speed stream pattern during this 6-month period following solar minimum is somewhat unusual since few large coronal holes were apparent and such an activity pattern is usually dominant in the solar wind during the declining phase of a cycle [*Crooker and Cliver,* 1994]. We note, however, that the wind speeds during this period were less than is typical during the declining phase, and the stream pattern was not recurrent.

Finally, the cause of the storm on March 29 is less obvious. A period of sustained but moderate southward field followed several days of higher speed flow. The southward field may have been associated with an interaction region or a small magnetic cloud.

In summary, we found a good association between the frontside halo CMEs and moderate storms with a lag time of 3–5 days. A similar result was reported by *Brueckner et al.* [1998] for the period March 1996 through June 1997. An even better association, 8 of 12, was found between magnetic clouds at Wind in front of Earth, with or without earlier halo CMEs, and the storms. All but one of the remaining four storms appeared to be caused by CIRs preceding high-speed streams passing by Earth.

4. Interplanetary Propagation of Disturbances

As a consistency check on halo CME and magnetic cloud associations, we used two techniques involving the transit speed of the disturbance to Wind compared with the in-situ speed observed at Wind. We will use the January 6–10 event as an example. The front of the magnetic cloud was detected at WIND on January 10 at 0445 UT preceded by an interplanetary shock arriving at 0100 UT. Using an extrapolated onset time of the CME and DF near Sun center after midday on January 6 yields a transit speed to the Wind cloud detection of 480 km s^{-1}. This speed is reasonably consistent with the average in-situ wind speed within the cloud of 435 km s^{-1}. We compared the source-to-cloud transit and in-situ wind speeds for all six frontside halo CME events with near-Sun center sources (Table 2). These speed pairs were all within 100 km s^{-1} of each other with a range from 10 to 100 km s^{-1}.

As an additional check, if we assume we know the solar onset time of a shock detected at Wind, we can calculate its transit time to Wind. These we can compare with the data set from *Cliver et al.* [1990] of the speeds of shocks with well- determined solar sources and the peak solar wind speeds observed at 1 AU. This technique was used by *Webb et al.* [1998b] for the January 1997 event to support the association of the cloud and storm on January 10–11 with the DF on January 6 rather than with a brighter long duration event (LDE) on the previous day. The data point for the January event is plotted as "2" on Figure 7, which is adapted from the Cliver et al. study.

On Figure 7 we have plotted the shock transit and in-situ wind speed points for all six frontside halo CME events. As for January 6, for each event, we calculated the transit time from the solar surface source to the shock arrival time at Wind and compared it with the

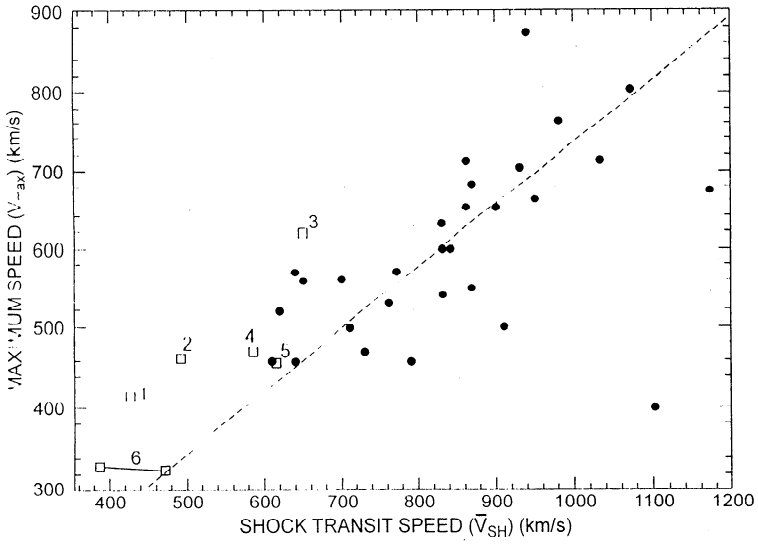

Figure 7. Plot of the maximum in-situ solar wind speed of disturbances with confidently identified solar sources and the associated shock transit speed adapted from *Cliver et al.* [1990]. The wind speeds and transit times associated with the six frontside halo CMEs of this study were measured relative to the associated interplanetary shocks detected at Wind. These data points are shown as open boxes with the numbers indicting the time order of the halo CME events from Table 2 (the March 9 event is not included because the source region was near the limb). The dashed line is the linear best-fit to the data points (filled circles) from the Cliver et al. study. Note that all the data points from this study lie above this line.

observed maximum solar wind speed behind the shock at 1 AU. The plot shows that all of the halo CME–shock data points cluster together and lie above the best-fit line from *Cliver et al* [1990]. There is also a tendency for these points to lie to the left of the Cliver et al. data, having slower transit speeds. This latter effect may be due to the difference in energy or speed between events occurring just after solar minimum (this study) and events during maximum phases (the Cliver et al. events). Although the general displacement between the two data sets is not understood, it may reflect a solar cycle dependence.

5. Discussion and Conclusions

In summary, the solar activity associated with the seven frontside halo CMEs typically had these characteristics: (1)) large-arc CMEs arising from surface activity near Sun center suggesting eruptive events aimed toward Earth, (2) surface events consisting of flares covering a range of energies associated with long-enduring coronal arcades within small emerging or rapidly evolving active regions, (3) coronal dimming regions likely due to local depletions of preexisting coronal density, (4) large-scale coronal waves (in all three events having sufficient EIT data), and (5) small but "important" erupting filaments.

During the 6 month post solar minimum period of this study, halo CMEs and geomagnetic storms occurred with similar frequencies, suggesting a close relationship: 14 halo CMEs and 12 moderate-level storms. As noted above, 7 of the 14 halo CMEs were associated with frontside surface activity. The activity for six of these seven occurred in active regions within 0.5 R_S of Sun center and thus were consistent with being Earthward-directed. In a remarkable confirmation, *all six Earthward-directed halo CMEs were associated with magnetic clouds and moderate storms at Earth 3–5 days later.*

Thus, halo CMEs associated with long-enduring surface activity within 0.5 R_S of Sun center appear to be an excellent indicator of increased geoactivity 3–5 days later. Note that this activity need not be intense, just aimed in the "right" direction. As expected, all but one of the geoeffective halo CMEs in our sample were nearly complete circles (i.e., had spans >290°, see Table 2). The exception was the partial halo CME on May 21, but it was associated with the active region closest to Sun center. Thus, even partial halo CMEs can be geoeffective if accompanied by surface activity near Sun center. It appears that shocks and magnetic clouds are also likely to be detected at Earth following such events.

The reason that any CME/magnetic cloud encountering Earth is likely to cause a storm is that geoeffective solar wind parameters, particularly sustained B_S fields, will probably occur within or ahead of any CME traveling within the heliosphere. As we found in our sample, the storm periods associated with the frontside halo CMEs closely tracked periods of strong, sustained southward fields either in the magnetic clouds or in the preceding post-shock regions. All but one of the halo CME–storms were associated with an interplanetary shock, consistent with the fact that greater-than-ambient wind speeds compress any existing southward IMF and thus increase the magnitude of the storms. Enhanced southward field behind interplanetary shocks has been noted before as an important cause of large storms [e.g., *Tsurutani et al.*, 1988; *Gosling et al.*, 1991]. In some cases the southward field ahead of the CME–cloud appears to have originated at the Sun as the overlying preexisting coronal fields that are ejected along with the CME [e.g., *Tsurutani et al.*, 1998].

Many of the storms were also associated with southward fields and enhanced flow speeds associated with CIRs and high-speed streams. CIRs are geoeffective because they compress and enhance preexisting southward fields and density in the gradient between slow and fast flows. Peak activity associated with several of the CME–storm events was also enhanced because the CME was superimposed on the CIR–high speed stream combination. Such combined events frequently contribute to the recurrence pattern of enhanced geoactivity that is most obvious during the declining phase of a cycle [*Crooker and Cliver*, 1994; *Tsurutani et al.*, 1995; *McAllister and Crooker*, 1997.]

The halo CMEs during this period occurred at rate of ~2 per month, or 0.08 per day. Overall the rates of occurrence of LASCO halo CMEs ranged from 0.045 d^{-1} in 1996 to 0.25 d^{-1} in 1998. During this period, halo CMEs comprised ~11% of all CMEs and tracked the CME rate. We can make a rough estimate of the fraction of all CMEs that would appear as halos if CMEs erupted randomly over all solar longitudes. Since the average CME width is ~50°, 50/360 or 14% of all CMEs might appear as halos along the Sun-Earth line. For the sake of this simplistic argument, we assume that LASCO has a 100% duty cycle and requires no visibility correction for CMEs viewed away from the skyplane, but we do not take into account any scattering or geometrical effects with respect to the skyplane. Given these caveats, the occurrence rate of halo CMEs during the time period of this study is roughly consistent with the rate expected if CMEs occur randomly in longitude across the Sun.

If frontside halo events are considered to be CMEs aimed directly at Earth, then analyses of data from near-Earth spacecraft in the solar wind should provide fundamental information on the physical structure of CMEs along their central axes. We found that all of the frontside halos arising near Sun center were associated with magnetic clouds and shocks in the Wind data at 1 AU. This is despite the fact that these events appeared to be relatively weaker as expected for near-solar minimum activity. Thus, it appears that shocks and magnetic clouds, possibly arising from filament-related flux ropes, appear to be characteristic of CMEs in general and that these features are most notable in this data set because we are sampling the CME material head on at 1 AU. Such flux ropes may be associated with deple-

tions of the coronal material at their feet. Therefore, in the future, we should be able to learn much about the internal structure of CMEs, and their interior magnetic clouds, through analyses of frontside halo CMEs.

It is interesting that two of the storms were associated with magnetic clouds that did not have obvious CMEs (halos or otherwise) or surface activity at the Sun. Because of the otherwise strong correspondence we found between halo CMEs and clouds at 1 AU, it seems likely to us that the CMEs were there but did not appear as halos surrounding the LASCO occulter. Possibilities are that the CMEs were too narrow in size, not dense enough along the line of sight, or not fast or energetic enough. This idea supports the argument of *Howard et al.* [1982] that only the densest or most energetic CMEs aimed along the Sun–Earth line could be seen as halos by the Solwind coronagraph. Thus LASCO, despite having increased sensitivity, might also have a limiting threshold below which head-on CMEs would not be detected. On the other hand, the rate calculation above argues that LASCO is not missing a significant number of CMEs, whether halo or not. Clearly, this question needs to be addressed with a much larger sample of halo events.

The May 21–27, 1997, halo CME-storm was a possible "toroidal" halo CME in that simultaneous activity was confined to the equator over both limbs of the Sun, with a faint band connecting them to the south. The assumption is that such a CME consists of a wide band surrounding the solar equator and expanding outward. We note that three of the four storms not clearly associated with frontside halo CMEs did have probable *backside* halo events occur within 5 days before the storms! We can speculate that occasionally a CME may encompass the eruption of a significant fraction of the coronal current sheet or multiple coronal arcades, such as has been observed in several Yohkoh soft X-ray events [*Webb et al.*, 1997b]. Depending on preexisting structures, transient material from such a CME could reach Earth from a wide range of source longitudes, causing unusually prolonged effects. However, such extremely wide CMEs must be rare, since the mean width of CMEs is only 50° and the occurrence rate of shocks and storms at Earth is not extraordinarily large. Thus, we are left with a rather puzzling result concerning the "global" nature of CMEs and their geoeffectiveness that requires further study.

Finally, we found that the source regions of the frontside halo CMEs involved small active regions which had been formed by recently emerging magnetic flux and were evolving relatively rapidly. The Hale polarities of these new regions were mixed between old-cycle and new-cycle polarity, as expected for this time period just after cycle minimum. Thus, our results appear to be consistent with CME models which require emerging or sheared flux as a driver or destabilization agent leading to a CME [e.g., *Linker and Mikic*, 1995; *Guo et al.*, 1996; *Antiochos et al.*, 1999].

Acknowledgments. This study is part of a collaboration between the ISTP and SHINE programs studying the solar sources of CMEs and their propagation through the interplanetary medium to Earth. SOHO is an international collaboration between NASA and ESA and is part of the ISTP. Yohkoh is a mission of the Institute of Space and Astronautical Science (Japan), with participation from the U.S. and U.K. We are grateful to J. Harvey of NSO/Kitt Peak and R. Lepping, the PI of the MFI experiment on Wind, for providing data and helpful discussions for this study. We also thank the referees for comments that improved the maunscript. DFW was supported by the Air Force Research Laboratory under contract AF19628–96–K–0030, by AFOSR grant AF49620–98–1–0062, and by NASA grant NAGW–4578; NUC was supported by NASA grant NAG5–7049 and NSF grant ATM–9805064; and OCS was supported by NASA contract S–86760–E.

Janet G. Luhmann thanks David Rust and another referee for their assistance in evaluating this paper.

References

Antiochos, S.K., C.R. DeVore, and J.A. Klimchuk, A model for solar coronal mass ejections, *Astrophys. J., 510,* 485, 1999.

Benevolenskaya, E.E., J.T. Hoeksema, A.G. Kosovichev, and P.H. Scherrer, The interaction of new and old magnetic fluxes at the beginning of solar cycle 23, *Astrophys. J., 517,* L163, 1999.

Berdichevsky, D. et al., Evidence for multiple ejecta: April 7–11, 1997, ISTP Sun-Earth connection event, *Geophys. Res. Lett., 25,* 2473, 1998.

Bothmer, V. and D. M. Rust, The field configuration of magnetic clouds and the solar cycle, in *Coronal Mass Ejections, Geophys. Monogr. Ser.,* vol. 99, edited by N. Crooker et al., p. 139, AGU, Washington, D.C., 1997.

Brueckner, G.E., et al., The large angle spectroscopic coronagraph (LASCO), *Solar Phys., 162,* 357, 1995.

Brueckner, G.E., et al., Geomagnetic storms caused by coronal mass ejections (CMEs): March 1996 through June 1997, *Geophys. Res. Lett., 25,* 3019, 1998.

Burlaga, L.F.E., Magnetic clouds, in *Physics of the Inner Heliosphere,* Vol. 2, edited by R. Schwenn and E. Marsch, p. 1, Springer-Verlag, New York, 1991.

Burlaga, L., et al., A magnetic cloud containing prominence material: January 1997, *J. Geophys. Res., 103,* 277, 1998.

Burton, R.K., R.L. McPherron and C.T. Russell, An empirical relationship between interplanetary conditions and *Dst, J. Geophys. Res., 80,* 4204, 1975.

Cane, H.V., I.G. Richardson and O.C. St. Cyr, The interplanetary events of January–May, 1997 as inferred from energetic particle data, and their relationship with solar events, *Geophys. Res. Lett., 25,* 2517, 1998.

Cane, H.V., I.G. Richardson and O.C. St. Cyr, Correction to "The interplanetary events of January–May, 1997 as inferred from energetic particle data, and their relationship with solar events" by H.V. Cane, I.G. Richardson, and O.C. St. Cyr, *Geophys. Res. Lett., 26,* 2149, 1999.

Cliver, E.W., J. Feynman, and H.B. Garrett, An estimate of the maximum speed of the solar wind, 1938–1989, *J. Geophys. Res., 95,* 17,103, 1990.

Crooker, N.U. and E.W. Cliver, Postmodern view of M-regions, *J. Geophys. Res., 99,* 22,383, 1994.

Crooker, N.U. and A.H. McAllister, Transients associated with recurrent storms, *J. Geophys. Res., 102,* 14,041, 1997.

Crooker, N.U., A.J. Lazarus, R.P. Lepping, K.W. Ogilvie, J.T. Steinberg, A. Szabo and T.G. Onzager, A two-stream, four-sector recurrence pattern: Implications from Wind for the 22-year geomagnetic activity cycle, *Geophys. Res. Lett., 23,* 1275, 1996.

Crooker, N.U., J.T. Gosling, and S.W. Kahler, Magnetic clouds at sector boundaries, *J. Geophys. Res., 103,* 301, 1998.

Fox, N.J., M. Peredo, and B.J. Thompson, Cradle-to-grave tracking of the January 6–11, 1997, Sun-Earth connection event, *Geophys. Res. Lett., 25,* 2461, 1998.

Gloeckler, G., L.A. Fisk, S. Hefti, N.A. Schwadron, T.H. Zurbuchen, F.M. Ipavich, J. Geiss, P. Bochsker, and R.F. Wimmer-Schweingruber, Unusual composition of the solar wind in the 2–3 May 1998 CME observed with SWICS on ACE, *Geophys. Res. Lett., 26,* 157, 1999.

Gosling, J.T., Corotating and transient solar wind flows in three dimensions, in *Annual Reviews of Astronomy and Astrophysics,* vol. 34, edited by G. Burbidge and A. Sandage, p. 35, Ann. Rev., Palo Alto, Calif., 1996.

Gosling, J.T., D.J. McComas, J.L. Phillips, and S.J. Bame, Geomagnetic activity associated with earth passage of interplanetary shock disturbances and coronal mass ejections, *J. Geophys. Res., 96,* 731, 1991.

Guo, W.P., S.T. Wu, and E. Tandberg-Hanssen, Disruption of helmet streamers by current emergence, *Astrophys. J., 469,* 944, 1996.

Harvey, K.L. and O.R. White, What is solar cycle minimum?, *J. Geophys. Res., 104,* 19,759, 1999.

Howard, R.A., D.J. Michels, N.R. Sheeley, Jr., and M.J. Koomen, The observation of a coronal transient directed at Earth, *Astrophys. J., 263,* L101, 1982.

Howard, R.A., et al., Observations of CMEs from SOHO LASCO, in *Coronal Mass Ejections, Geophys. Monogr. Ser.,* vol. 99, edited by N. Crooker, J. Joselyn and J. Feynman, p. 17, AGU, Washington, D.C., 1997.

Hudson, H.S. and D. F. Webb, in *Coronal Mass Ejections, Geophys. Monogr. Ser.,* vol. 99, edited by N. Crooker et al., p. 27, AGU, Washington, D.C., 1997.

Hudson, H.S., J.R. Lemen, O.C. St. Cyr, A.C. Sterling, and D. F. Webb, X-ray coronal changes during halo CMEs, *Geophys. Res. Lett., 25,* 2481, 1998.

Jackson, B.V., Helios observations of the Earthward-directed mass ejection of 27 November, 1979, *Solar Phys., 95,* 363, 1985.

Kahler, S.W., The morphological and statistical properties of solar X-ray events with long decay times, *Astrophys. J., 214,* 891, 1977.

Kahler, S.W., Solar flares and coronal mass ejections, *Annu. Rev. Astron. Astrophys., 30,* 113, 1992.

Lepping, R.P., J.A. Jones, and L.F. Burlaga, Magnetic field structure of interplanetary magnetic clouds at 1 AU, *J. Geophys. Res., 95,* 11,957, 1990.

Linker, J.A. and Z. Mikic, Disruption of a helmet streamer by photospheric shear, *Astrophys. J., 438,* L45, 1995.

Loewe, C.A. and G.W. Prolss, Classification and mean behavior of magnetic storms, *J. Geophys. Res., 102,* 14,209, 1997.

Lyons, M.A., B.J. Thompson, O.C. St. Cyr, D. Berdichevsky, S.P. Plunkett, R.A. Howard, and J.T. Burkepile, An investigation of different methods of determining the potential geospace impact of CMEs, *Eos Trans. AGU, 79*(46), Fall Meet. Suppl., F718, 1998.

McAllister, A.H., and N.U. Crooker, Coronal mass ejections, corotating intercation regions, and geomagnetic storms, in *Coronal Mass Ejections, Geophys. Monogr. Ser.,* vol. 99, edited by N. Crooker et al., p. 279, AGU, Washington, D.C., 1997.

Michels, D.J., R.A. Howard, M.J. Koomen, S. Plunkett, G.E. Brueckner, Ph. Lamy, R. Schwenn, and D.A. Biesecker, Visibility of Earth-directed coronal mass ejections, in *The Corona and the Solar Wind Near Minimum Activity,* ESA SP–404, p. 567, ESTEC, Noordwijk, The Netherlands, 1997.

Munro, R.H., J.T. Gosling, E. Hildner, R.M. MacQueen, A.I. Poland, and C.L. Ross, The association of coronal mass ejections with other forms of solar activity, *Solar Phys., 61,* 201, 1979.

Reiner, M.J., M.L. Kaiser, J. Fainberg, J.-L. Bougeret, and R.G. Stone, On the origin of radio emissions associated with the January 6–11, 1997, CME, *Geophys. Res. Lett., 25,* 2493, 1998.

Sheeley, N.R., Jr., R.A. Howard, M.J. Koomen, and D.J. Michels, Associations between coronal mass ejections and soft X-ray events, *Astrophys. J., 272,* 349, 1983.

Skoug, R.M., et al., A prolonged He^+ enhancement within a coronal mass ejection in the solar wind, *Geophys. Res. Lett., 26,* 161, 1999.

Smith, Z., S. Watari, M. Dryer, P.K. Manoharan, and P.S. McIntosh, Identification of the solar source for the 18 October 1995 magnetic cloud, *Solar Phys., 171,* 177, 1997.

Solar–Geophysical Data Bulletins, Natl. Oceanic and Atmos. Admin., WDC-A, Boulder, Colo., 1997-1999.

St. Cyr, O.C. and A. J. Hundhausen, On the interpretation of "halo" coronal mass ejections, in *Proceedings of the Sixth International Solar Wind Conference,* vol. 1, edited by V.J. Pizzo, T.E. Holzer and D.G. Sime, p. 235, Natl. Cent. for Atmos. Res., Boulder, Colo., 1988.

St. Cyr, O.C. and D.F. Webb, Activity associated with coronal mass ejections at solar minimum: SMM observations from 1984–1986, *Solar Phys., 136,* 379, 1991.

Sterling, A.C., and H.S. Hudson, Yohkoh SXT observations of X-ray "dimming" associated with a halo coronal mass ejection, *Astrophys. J., 491,* L55, 1997.

Thompson, B.J., S.P. Plunkett, J.B. Gurman, J.S. Newmark, O.C. St. Cyr and D.J. Michels, SOHO/EIT observations of an Earth-directed coronal mass ejection on May 12, 1997, *Geophys. Res. Lett., 25,* 2465, 1998.

Thompson, B.J., O.C. St. Cyr, S.P. Plunkett, J.B. Gurman, N. Gopalswamy, H.S. Hudson, R.A. Howard, D.J. Michels, and J.-P. Delaboudiniere, The correspondence of EUV and white light observations of coronal mass ejections with SOHO EIT and LASCO, in *Sun-Earth Plasma Connections, Geophys. Monogr. Ser.,* vol. 109, edited by J. L. Burch, R. L. Carovillano, and S. K. Antiochos, p. 31, AGU, Washington, D.C., 1999a.

Thompson, B.J., et al., SOHO/EIT observations of the 1997 April 7 coronal transient: Possible evidence of coronal moreton waves, *Astrophys. J., 517,* L151, 1999b.

Tsurutani, B.T., W.D. Gonzalez, F. Tang, S.I. Akasofu, and E.J. Smith, Origin of interplanetary southward magnetic fields responsible for major magnetic storms near solar maximum (1978–1979), *J. Geophys. Res., 93,* 8519, 1988.

Tsurutani, B.T., W.D. Gonzalez, A.L.C. Gonzalez, and F. Tang, Interplanetary origin of geomagnetic activity in the declining phase of the solar cycle, *J. Geophys. Res., 100,* 21,717, 1995.

Tsurutani, B.T., et al., The January 10, 1997 auroral hot spot, horseshoe aurora and first substorm: A CME loop?, *Geophys. Res. Lett., 25,* 3047, 1998.

Webb, D.F., The solar sources of coronal mass ejections, in *Eruptive Solar Flares,* edited by Z. Svestka, B.V. Jackson, and M.E. Machado, p. 234, Springer-Verlag, New York, 1992.

Webb, D.F., CMEs and prominences and their evolution over the solar cycle, in *New Perspectives on Solar Prominences,* edited by D. Webb, D. Rust and B. Schmieder, p. 463, *ASP Conf. Ser.,* vol. 150, Astron. Soc. of the Pac., San Francisco, Calif., 1998.

Webb, D.F. and A.J. Hundhausen, Activity asociated with the solar origin of coronal mass ejections, *Solar Phys., 108,* 383, 1987.

Webb, D.F. and B.V. Jackson, The identification and char-

acteristics of solar mass ejections observed in the heliosphere by the Helios 2 photometers, *J. Geophys. Res., 95,* 20,641, 1990.

Webb, D., E. Cliver, N. Crooker, and O. St. Cyr, Halo CMEs and the characteristics of related geoactivity, *Eos Trans. AGU, 78*(46), Fall Meet. Suppl., F533, 1997a.

Webb, D.F., S.W. Kahler, P.S. McIntosh, and J.A. Klimchuk, Large-scale structures and multiple neutral lines associated with coronal mass ejections, *J. Geophys. Res., 102,* 24,161, 1997b.

Webb, D., E. Cliver, N. Crooker, and O. St. Cyr, Halo CMEs as a predictor of space weather, presented at *32nd Scientific Assembly of COSPAR, Abstract Book,* p. 243, COSPAR Secretariat, Nagoya, Japan, 1998a.

Webb, D.F., E.W. Cliver, N. Gopalswamy, H.S. Hudson, and O.C. St. Cyr, The solar origin of the January 1997 coronal mass ejection, magnetic cloud and geomagnetic storm, *Geophys. Res. Lett., 25,* 2469, 1998b.

Webb, D.F., R.P. Lepping, L.F. Burlaga, C.E. DeForest, D.E. Larson, S.F. Martin, S.P. Plunkett, and D.M. Rust, The origin and development of the May 1997 magnetic cloud, *J. Geophys. Res.*, in press, 2000.

N. U. Crooker, Center for Space Physics, 725 Commonwealth Ave., Boston University, Boston, MA 02215.

O. C. St. Cyr, CPI/Naval Research Laboratory, Code 682, NASA Goddard Space Flight Center, Greenbelt, MD 20771.

B. J. Thompson, Code 682, NASA Goddard Space Flight Center, Greenbelt, MD 20771.

D. F. Webb and E. W. Cliver, AFRL/VSBS, 29 Randolph Road, Hanscom AFB, MA 01731-3010 (e-mail: webb@plh.af.mil).

(Received July 23, 1999; revised October 19, 1999; accepted November 11, 1999.)